Protecting remote bipartite entanglement against amplitude damping by local unitary operations

Xiao-Lan Zong,[1] Chao-Qun Du,[1] Ming Yang,[1,*] Qing Yang,[1] and Zhuo-Liang Cao[1,2,†]
[1]*Key Laboratory of Opto-electronic Information Acquisition and Manipulation, Ministry of Education, School of Physics and Material Science, Anhui University, Hefei 230601, People's Republic of China*
[2]*School of Electronic and Information Engineering, Hefei Normal University, Hefei 230601, People's Republic of China*
(Received 25 July 2014; published 30 December 2014)

Remote entanglement will inevitably decrease due to the interactions between quantum systems and their environments. Therefore protecting remote entanglement against decoherence is of great importance in realizing quantum communication and quantum comp utation. In this paper, we demonstrate that decoherence caused by weak-measurement-induced damping can be effectively suppressed by adding local unitary operation series on each qubit. The results show that the entanglement of the output state can approach that of the state before amplitude damping. The most distinct advantage of this entanglement protection scheme is that any unitary operation (except the identity operation) has this entanglement reversal effect on the amplitude-damped states. Furthermore, in each local unitary operation series, all the operations can be different from one other, and all the time intervals between any two adjacent operations can be different too. In addition, there is no need for the two remote users to synchronize their operations. Unlike most of the previous schemes, we do not assume the instantaneous local unitary operation, and each operation has a duration. All these advantages suggest that this remote entanglement protection scheme is much simpler and feasible than the previous ones, and we hope it can be implemented in the near future. Recently, Y. S. Kim *et al.* [Nat. Phys. **8**, 117 (2012)] pointed out that "pre-weak measurement + amplitude damping + bit-flipping operation + post-weak measurement" can actively combat specific decoherence. By combing our proposal with Kim *et al.*'s scheme, the protection performance can be greatly improved by replacing the bit-flipping operation with an arbitrary rotational operation around the x axis, the number of the operations as well as the interval between any two adjacent operations all can be different, and the application range of the scheme can be greatly broadened.

DOI: 10.1103/PhysRevA.90.062345 PACS number(s): 03.67.Pp, 03.65.Ud, 03.67.Hk, 42.50.Lc

I. INTRODUCTION

Quantum entanglement is a crucial resource in quantum information and quantum computation, and it is also a noteworthy feature that can distinguish the quantum realm from the classical one [1]. However, the inevitable coupling of the quantum system with its environment will lead to quantum decoherence. Up to now, protecting entanglement against decoherence has aroused wide concern, and a number of strategies have been proposed for decoherence suppression, such as quantum error correction [2,3], decoherence-free subspace [4–6], dynamical decoupling [7,8], the quantum Zeno effect [9–11], and so on. In fact, depolarization, amplitude damping, and phase damping can cause quantum decoherence. In this paper, we focus only on amplitude damping, which occurs in many practical quantum systems [12], for example, an atomic qubit suffering from spontaneous decay, a superconducting qubit subjected to zero-temperature energy relaxation, a photon qubit in a leaky cavity, and so on.

Weak measurement is different from the typical Von Neumann quantum measurement, and many recent works showed that weak measurement can protect entanglement from decoherence. For instance, it was pointed out that weak measurements together with quantum measurement reversal could effectively protect a single-qubit state system from decoherence [13–15], and this idea could be extended to two-qubit systems [16] or even higher-dimensional systems [17]. What's more, these probabilistic reversal schemes were recently experimentally implemented in several quantum systems [18–21]. Then Sun *et al.* showed that weak measurement together with bit flip could also protect a state against amplitude damping [22]. Similarly, Wang *et al.* proposed a feed-forward scheme for protecting a quantum state against amplitude damping [23]. Al-Amri *et al.* showed that by introducing auxiliary qubits and Hadamard and controlled NOT (CNOT) gates one could probabilistically recover an arbitrary one-qubit or two-qubit state from damping with the help of weak measurement [24,25].

All current entanglement reversal (protection) schemes consider cases with perfectly accurate quantum operations. But any real quantum operation has its own level of accuracy, which will inevitably affect the efficiency of the entanglement protection schemes. Is it possible to efficiently protect entanglement via real quantum operations, i.e., quantum operations with some accuracy less than unity? We will give a positive answer to this question in this paper. In addition, Kim *et al.*'s scheme [20] only works for the case where the magnitude of the system decoherence, the strength of the weak measurement, and the strength of the reversing measurement satisfy a specific relation. But, in a real situation, it is not possible to know the magnitude of system decoherence, so in this paper, we want to release this condition too and design protection schemes for quantum states with a general decoherence rate.

This paper is organized as follows. In Sec. II we give a brief introduction of amplitude damping and weak measurement. In

*Corresponding author: mingyang@ahu.edu.cn
†zlcao@ahu.edu.cn

Sec. III, we consider the entanglement dynamics of a bipartite quantum system under amplitude damping, where an idea detector is introduced to monitor the environment; that is, we only consider the case where there is no excitation in the environment. We design a protection scheme for this special kind of amplitude-damped state by introducing a series of unitary operations on each qubit. In order to put forward a more practical protection scheme, here, we suppose that each operation is different from the others in the series and that the time intervals between any two adjacent operations are different too. These differences are characterized by random fluctuations around some fixed amplitude of local operations and some time interval between two operations, and we consider two different kinds of random fluctuation distributions: uniform distribution and Gaussian distribution. Based on the protection schemes in Sec. III, we modify Kim *et al.*'s scheme by replacing the bit-flipping operation with an arbitrary rotational operation around the x axis in Sec. IV. Four different modified schemes are proposed to protect the bipartite quantum system from the general amplitude damping (without monitoring the environment) with higher efficiencies. Section V summarizes the main results of the scheme and makes some conclusions.

II. AMPLITUDE DAMPING AND WEAK MEASUREMENT

Amplitude damping is a typical noise model describing system dissipation induced by the interaction between the quantum system and its environment, which can be understood as the transfer of excitation from the quantum system to its environment. Take a two-level atom as an example and suppose its environment is in the vacuum state initially; then the amplitude damping process can be described by the following map [12]:

$$\begin{aligned} &|0\rangle_S|0\rangle_E \to |0\rangle_S|0\rangle_E, \\ &|1\rangle_S|0\rangle_E \to \sqrt{1-p}|1\rangle_S|0\rangle_E + \sqrt{p}|0\rangle_S|1\rangle_E, \end{aligned} \tag{1}$$

where $p \in [0,1]$ is the probability of losing the system excitation to the environment and $\sqrt{1-p} = e^{-\gamma t}$, with γ being the decay rate. The subindices S, E denote the system and its environment, respectively.

Weak measurement is different from amplitude damping in the sense that an ideal detector is added to monitor the environment. The detector clicks with a probability p, indicating an excitation in the environment. But whenever there is an excitation in the environment, we will discard the result [22]. Thus the weak measurement can be represented by the following map:

$$\begin{aligned} &|0\rangle_S|0\rangle_E \to |0\rangle_S|0\rangle_E, \\ &|1\rangle_S|0\rangle_E \to \sqrt{1-p}|1\rangle_S|0\rangle_E. \end{aligned} \tag{2}$$

III. WEAK-MEASUREMENT-INDUCED DAMPING AND ITS REVERSAL

Assume two qubits A and B are initially prepared in extended Bell-like (EBL) states:

$$\rho_\phi = a|\phi\rangle\langle\phi| + \frac{1-a}{4}I, \quad |\phi\rangle = \mu|0_A0_B\rangle + \nu|1_A1_B\rangle, \tag{3}$$

where a varies from 0 to 1, μ and ν are complex numbers satisfying $|\mu|^2 + |\nu|^2 = 1$, and I is a 4×4 identity operation. In this paper, we choose $\mu = \nu = \frac{\sqrt{2}}{2}$ for simplicity.

To show how the decoherence map in Eq. (2) affects the EBL state, we consider identical weak measurements for both sides. Take the two-level atomic system as an example; this weak-measurement-induced damping process on each side can be described by the following Hamiltonian [26]:

$$H_{wk} = \tfrac{1}{2}\hbar\omega_0\sigma_z - i\gamma|1\rangle\langle 1|, \tag{4}$$

where $\sigma_z = |0\rangle\langle 0| - |1\rangle\langle 1|$, ω_0 is the atomic transition frequency, and γ is the spontaneous emission rate of level $|1\rangle$. In order to simplify the calculations, we can set $\hbar = 1$, and then one-qubit weak-measurement-induced evolution can be written as a nonunitary quantum operation in the interaction picture:

$$U_{wk}(t) = \begin{pmatrix} 1 & 0 \\ 0 & e^{-\gamma t} \end{pmatrix}. \tag{5}$$

The unnormalized density operator of the two qubits at time t is

$$\rho_\phi(t) = [U^1_{wk}(t) \otimes U^2_{wk}(t)]\rho_\phi[U^1_{wk}(t) \otimes U^2_{wk}(t)]^\dagger, \tag{6}$$

where $U^i_{wk}(t)\,(i = 1,2)$ is the weak measurement on the ith qubit. Here we choose Wootters' formula: concurrence [27] as an entanglement measure to quantify the entanglement between two qubits. By definition, the concurrence of quantum state ρ is expressed as

$$C(\rho) = \max(0, \sqrt{\lambda_1} - \sqrt{\lambda_2} - \sqrt{\lambda_3} - \sqrt{\lambda_4}), \tag{7}$$

where $\sqrt{\lambda_i}$ are the square roots of the eigenvalues in decreasing order of the matrix $\rho(\sigma_y \otimes \sigma_y)\rho^*(\sigma_y \otimes \sigma_y)$, with σ_y being the Pauli matrix. As depicted in Fig. 1, in the absence of any operation, the two remote qubits will inevitably suffer from weak-measurement-induced damping, which will decrease the entanglement quickly.

Now let's introduce our protection scheme, which can protect entanglement against decoherence by unitary operation series. As shown in Fig. 2, there exist two degrees of freedom in the unitary operation series: each unitary operation itself and the time interval between two adjacent operations.

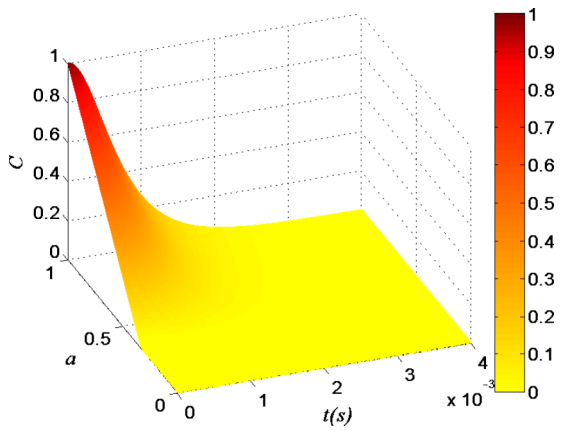

FIG. 1. (Color online) The concurrence $C(\rho_\phi(t))$ of two qubits is plotted as a function of t and a without control pulses. $\gamma = 1000$.

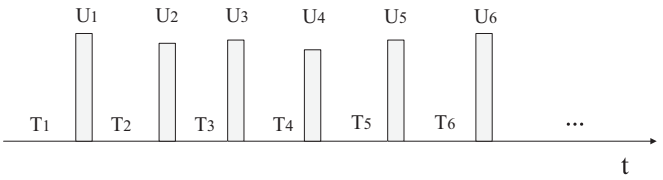

FIG. 2. Pulse distribution. T_i are the pulse intervals, and U_i represent the pulse series.

Next, we discuss the protection efficiency from these two aspects.

A. Entanglement protection via uniform and instantaneous pulse series

As shown in Fig. 2, to protect bipartite remote entanglement from amplitude damping, a control operation series will be added on each subsystem. In this section, we consider a simplified protection scheme where the control operation series are supposed to be instantaneous, identical, and uniformly distributed on the time axis. In our protection scheme, these local single-qubit operations can be described by the following unitary matrix:

$$U_\theta = \begin{pmatrix} \cos\theta & -i\sin\theta \\ -i\sin\theta & \cos\theta \end{pmatrix}, \tag{8}$$

where θ ranges from 0 to 2π. The reason why we choose this specific form of unitary transformation is that this kind of transformation on atomic states can be realized by resonant classical field driving [28]. This point will be explicitly discussed in Sec. III B, in which the control operations are not instantaneous. Suppose the interval between two neighboring pulses is T and the duration of each pulse is τ. In this section, $\tau \to 0$. The system evolution operator during an elementary cycle $[t_{N-1} = (N-1)(T+\tau), t_N = N(T+\tau)]$ is described by the following unitary operator:

$$U_C \equiv U(t_{N-1}, t_N) = U_\theta^{12} U_{wk}^{12}, \tag{9}$$

where $U_{wk}^{12} = U_{wk}^1(T) \otimes U_{wk}^2(T)$, $U_\theta^{12} = U_\theta^1 \otimes U_\theta^2$ [U_θ^i $(i = 1,2)$ is the unitary operator on the ith atom]. The evolution operator until $t_N = N(T+\tau)$ can be expressed by $U(t_N) = (U_C)^N$. Therefore the unnormalized density matrix at time $t = t_N + \bar{t}$ $(0 \leqslant \bar{t} < T)$ is

$$\rho_\phi(t_N + \bar{t}) = U_{wk}^{12}(\bar{t})(U_C)^N \rho_\phi((U_C)^N)^\dagger (U_{wk}^{12}(\bar{t}))^\dagger. \tag{10}$$

For the case of a pure initial state with $a = 1.0$, if the pulse interval is 10^{-4} s, the entanglement dynamics is modified by a train of unitary operations, and the concurrence of the two-qubit state is plotted in Fig. 3 as a function of time t and the unitary operation parameter θ. From Fig. 3, we can see that the disentanglement caused by amplitude damping can be prevented effectively with a wide range of unitary operations θ, and some special unitary operations can even stabilize the entanglement at the initial value.

From Fig. 4, we can see that the smaller the pulse interval is, the larger the range of the effective unitary operation θ is, and there are only three invalid operations (0, π, 2π; Fig. 5), i.e., identity operations. Meanwhile, we can see from Fig. 6 that the

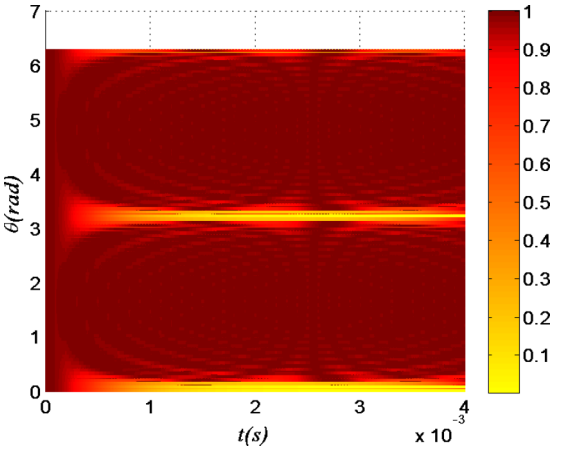

FIG. 3. (Color online) Contour plot of concurrence as a function of t and θ when a train of identical unitary operations is present. $a = 1.0$, $\gamma = 1000$, and the pulse interval T is 10^{-4} s.

probability of successfully protecting entanglement decreases with time. This can be understood as follows. Although the pulse series and the weak measurement can protect the entanglement, the global damping factor still exists, which causes the damping of the success probability for entanglement protection.

Up to now, we only considered the special pure-initial-state case with $a = 1$. It is of great importance to see whether or not our scheme still works for mixed initial states (for example, $a = 0.5$). The results show that this scheme works for mixed initial states too; the protection efficiency is similar to that of the pure-initial-state case.

B. Entanglement protection via nonuniform and noninstantaneous pulse series

In real situations, it is impossible to generate the same pulse for every control cycle, so we take the accuracy of operation into account. Consider the situation where there are fluctuations in the pulse intensities, and thus the corresponding unitary operations will not be identical. Within the current

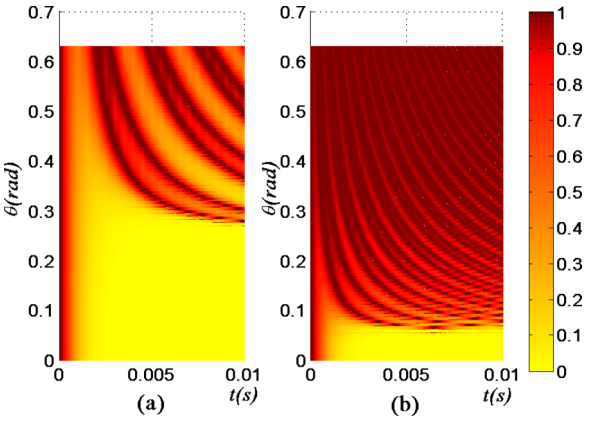

FIG. 4. (Color online) Contour plots of concurrence ($a = 1.0$, $\gamma = 1000$, $\theta \in [0, 0.2\pi]$). (a) The pulse interval T is 5×10^{-4} s. (b) The pulse interval T is 1×10^{-4} s.

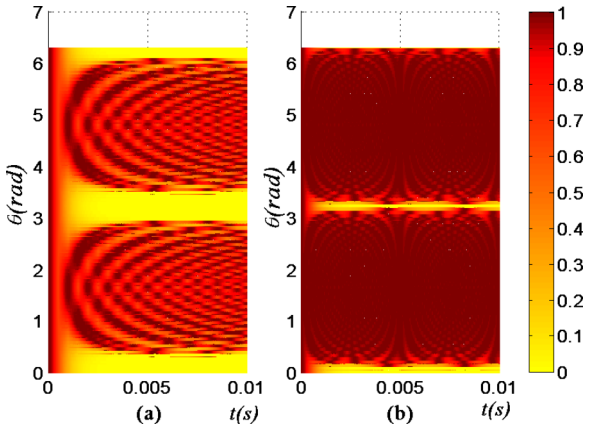

FIG. 5. (Color online) Contour plots of concurrence ($a = 1.0$, $\gamma = 1000$, $\theta \in [0,2\pi]$). (a) The pulse interval T is 5×10^{-4} s. (b) The pulse interval T is 1×10^{-4} s.

technology, we can assume a fluctuation of the order of 10% among the operations. In addition, the time intervals cannot be precisely equal to each other, which will induce a fluctuation around some fixed time interval too. Here we are going to consider two different kinds of random fluctuation distributions for comparison: uniform distribution and Gaussian distribution. First, we consider the case of uniform random fluctuation. According to numerical simulation, we can see clearly from Fig. 7 that our scheme still works fine even though the operations are not perfect. Similarly, if there is a fluctuation of the order of 10% among the time intervals, our scheme still can protect entanglement well (Fig. 8). A comparison between Figs. 7 and 8 shows that the pulse intensity fluctuation has a greater impact on the protection scheme than the time interval fluctuation. In order to clarify this point, we plot Fig. 9 with $\theta = 0.25\pi$. If the two above-mentioned fluctuations occur simultaneously, what will happen to our protection scheme? As shown in Fig. 10(a), the numerical simulation shows that our protection scheme still works fine under the combination of these two fluctuations. Up to now, our protection scheme works fine in the presence of both a time interval and pulse intensity fluctuations in a uniform random distribution. One may wonder whether our scheme still works fine when the random fluctuation is in a Gaussian distribution. A comparison

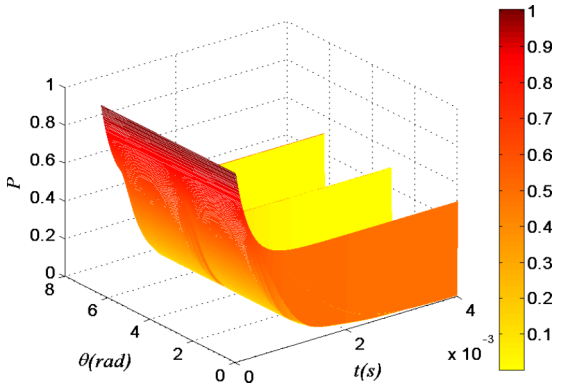

FIG. 6. (Color online) The probability of protecting entanglement. $a = 1.0$, $\gamma = 1000$, and the pulse interval T is 10^{-4} s.

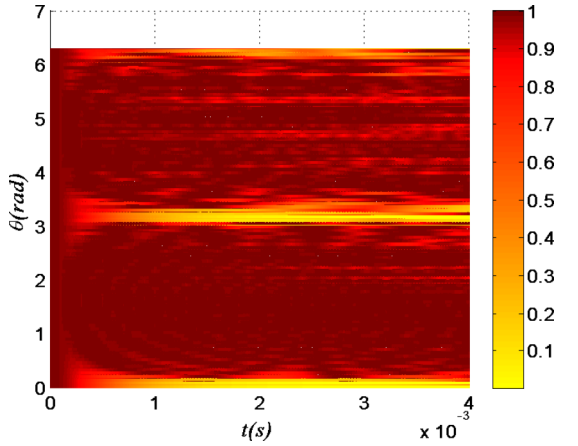

FIG. 7. (Color online) Contour plot of concurrence as a function of t and θ when the unitary operations are not identical. The uniform random fluctuation values range from -0.1θ to 0.1θ. $a = 1.0$ $\gamma = 1000$, and the pulse interval T is 10^{-4} s.

between Figs. 10(a) and 10(b) shows that the uniform random fluctuation has a greater impact on the result than the Gaussian random fluctuation, which can be understood as follows. The mean value of the Gaussian distribution is zero, and thus the fluctuation values are most likely distributed closely around the mean value of zero rather than the uniformly distributed fluctuation values in the uniform-random-fluctuation case. In addition, if we reduce the standard deviation of the Gaussian distribution, the protection effects will improve, as shown in Fig. 11.

Until now, the unitary operations are assumed to be instantaneous, but this situation is not going to happen in the laboratory. That is to say, during the pulse operation, the state is still suffering from damping. Thus, besides the time interval and the pulse intensity fluctuations, we need to take the pulse duration ($\tau \neq 0$) into account too. During the operation pulse duration τ, the system still suffers from weak-measurement-induced damping. Thus, by including the weak-measurement-induced damping during a local unitary operation, the total evolution

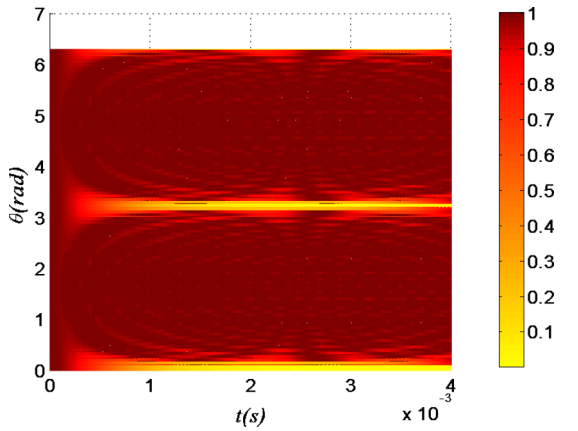

FIG. 8. (Color online) Contour plot of concurrence as a function of t and θ when the time intervals are not identical. The uniform random fluctuation values range from $-0.1T$ to $0.1T$. $a = 1.0$, $\gamma = 1000$, and the ideal pulse interval T is 10^{-4} s.

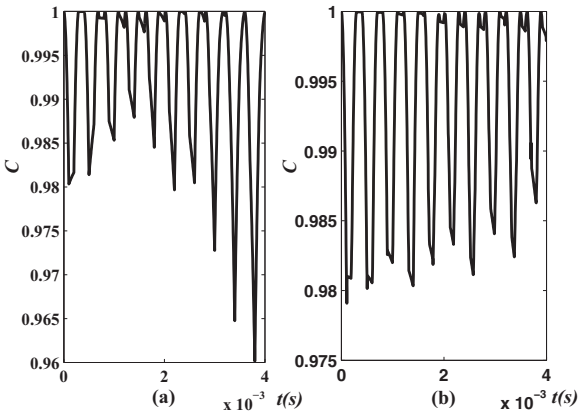

FIG. 9. The concurrence as a function of t. $a = 1.0$ and $\gamma = 1000$. (a) The operation parameter θ fluctuates around 0.25π, the fluctuation values are uniformly distributed over a range of $-0.1 \times 0.25\pi$ to $0.1 \times 0.25\pi$, and the ideal pulse interval is 10^{-4} s. (b) There are fluctuations in the time interval, the fluctuation values are uniformly distributed over a range of -0.1×10^{-4} to -0.1×10^{-4} s, and $\theta = 0.25\pi$.

of the system during the pulse duration τ can be governed by a non-Hermitian Hamiltonian [28]:

$$H = \tfrac{1}{2}\hbar\omega_0\sigma_z - i\gamma|1\rangle\langle 1| + \hbar\Omega(S^+e^{-i\omega_L t} + S^-e^{i\omega_L t}), \quad (11)$$

where the last term describes the driving by a classical field, Ω is the coupling constant, ω_L is the frequency of the driving field, $S^+ = |1\rangle\langle 0|$, and $S^- = |0\rangle\langle 1|$. For the resonant driving case $\omega_0 = \omega_L$, the system evolution is governed by the following Hamiltonian in the interaction picture:

$$H^I = -i\gamma|1\rangle\langle 1| + \Omega(S^+ + S^-). \quad (12)$$

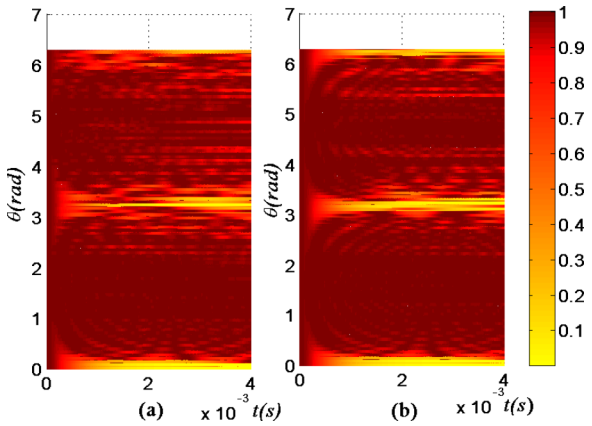

FIG. 10. (Color online) Contour plots of concurrence as a function of t and θ when there are fluctuations both in the time intervals and in the pulse intensities. The time interval values fluctuate from $-0.1T$ to $0.1T$ with the central value 10^{-4} s, and the operation parameters fluctuate from -0.1θ to 0.1θ. $a = 1.0$, $\gamma = 1000$. (a) The random fluctuation is in the uniform distribution. (b) The random fluctuation is in Gaussian distribution with the mean value $\mu = 0$ and the standard deviation $\sigma = 0.05$.

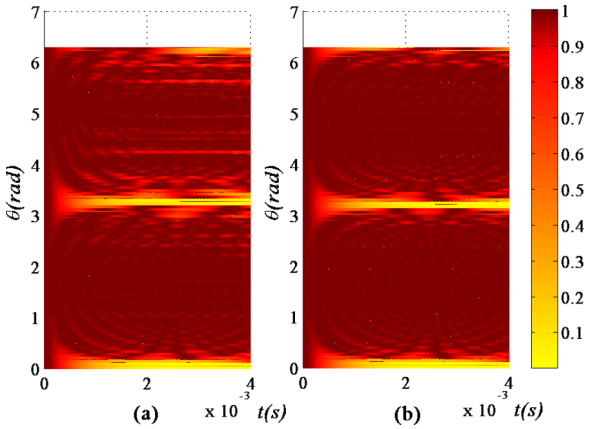

FIG. 11. (Color online) Contour plots of concurrence as a function of t and θ when there are fluctuations both in the time intervals and in the pulse intensities. The time interval values fluctuate from $-0.1T$ to $0.1T$ with the central value 10^{-4} s, and the operation parameters fluctuate from -0.1θ to 0.1θ. $a = 1.0$, $\gamma = 1000$. The random fluctuations of these two parameters are all in Gaussian distribution with the mean value $\mu = 0$. (a) The standard deviation $\sigma = 0.05$. (b) The standard deviation $\sigma = 0.01$.

The detailed evolution operator induced by this Hamiltonian is too complicated, so it is not presented here. Here, to incorporate the effects of real fluctuations on the local operations, the fluctuations of both pulse intensity and pulse duration must be considered. Without loss of generality, we can assume that the coupling constant Ω is fixed, and there are fluctuations only in the pulse duration. With the coupling constant being fixed, the local control operation varies with the driving time of each control pulse. That is to say, different pulse durations τ correspond to different control operations. So, in Fig. 12,

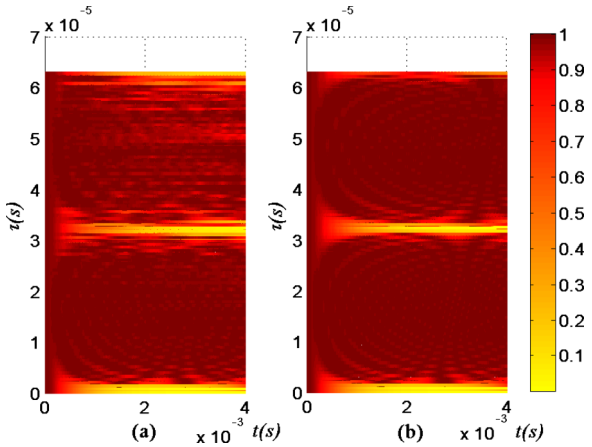

FIG. 12. (Color online) Contour plot of concurrence as a function of t and τ, where the pulse duration τ of the local operation is incorporated and there are fluctuations both in the time intervals and in the pulse durations. The time interval values fluctuate from $-0.1T$ to $0.1T$ with the central value 10^{-4} s, and the pulse duration τ fluctuates from -0.1τ to 0.1τ. $a = 1.0$, $\gamma = 1000$, $\Omega = 100000$. (a) The random fluctuation is in uniform distribution. (b) The random fluctuation is in Gaussian distribution with the mean value $\mu = 0$ and the standard deviation $\sigma = 0.05$.

the concurrence of a two-atom state is plotted as a function of time t and the pulse duration τ, which shows that our scheme still works fine when the control pulse duration is less than $0.3T$.

IV. AMPLITUDE DAMPING AND ITS REVERSAL

In Sec. III, we considered only the protection scheme for the states under weak-measurement-induced damping. If the environment is not continuously monitored by a detector, how do we protect the states from amplitude damping? Kim *et al.* showed that the decoherence caused by amplitude damping can be suppressed by implementing a weak measurement and the reversing measurement before and after the damping channel [20]. The physical mechanism behind this scheme is that a prior weak measurement intentionally moves the initial state closer to its ground state, which does not experience amplitude-damping decoherence. Therefore the entanglement is naturally preserved. In fact, the reversing measurement is equivalent to the instantaneous bit-flipping operation plus a weak measurement, so Kim *et al.*'s scheme can be expressed as pre-weak measurement + amplitude damping + bit-flipping operation + post-weak measurement, as depicted in Fig. 13(a).

Here we show that implementing only one bit-flipping operation before post-weak measurement is not optimal. Instead of the bit-flipping operation, consider the rotation operation about the $\hat{x}$ axis (U_θ), which is described by Eq. (8). When $\theta = \pi/2$, U_θ represents the bit-flipping operation. Using this rotational operation, we give four

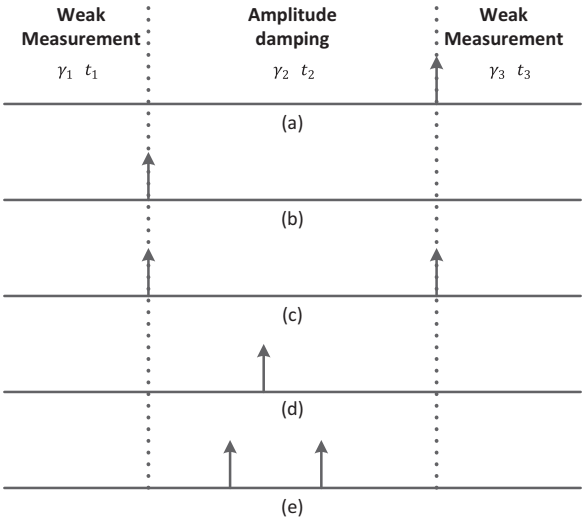

FIG. 13. Kim *et al.*'s protection scheme and our four different modifications. (a) Kim *et al.*'s scheme: a bit-flipping operation is applied at the end of amplitude damping. (b) Scheme 1: a rotational operation is performed before amplitude damping. (c) Scheme 2: two rotational operations are applied, one before and one after amplitude damping. (d) Scheme 3: one rotational operation is added at a random time point during the amplitude damping. (e) Scheme 4: two rotation operations are added at two random time points during the amplitude damping. γ_i and t_i, $i = 1,2,3$, are decay rates and duration times for three segments, respectively.

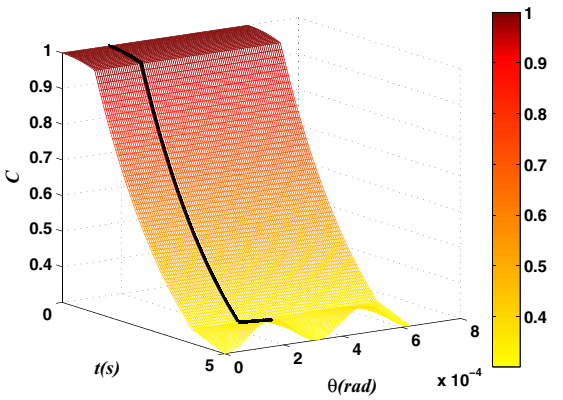

FIG. 14. (Color online) Concurrence evolution in Kim *et al.*'s scheme as a function of time t and θ. The black line is optimum, and the corresponding $\theta = \pi/2$. $\gamma_1 = 1000, t_1 = 10^{-4}$ s, $\gamma_2 = 1000, t_2 = 6 \times 10^{-4}$ s, $\gamma_3 = 2077, t_3 = 10^{-1}$ s, and total time is 8×10^{-4} s. $a = 1.0$.

different modifications to Kim *et al.*'s scheme. The first modification can be expressed as pre-weak measurement + rotation operation + amplitude damping + post-weak measurement [Fig. 13(b)], and the second one is expressed as pre-weak measurement + rotation operation + amplitude damping + rotation operation + post-weak measurement [Fig. 13(c)]. Figures 13(d) and 13(e) represent our third and fourth modifications, where one or two rotation operations are added at random time points during the amplitude-damping process.

Comparing Fig. 14 with Fig. 15, we find that the bit-flipping operation is optimal in Kim *et al.*'s scheme, while in our first modification [Fig. 13(b)], the optimal operation parameter is $\theta = 6\pi/25$. In Fig. 16, the black solid line represents the concurrence evolution in Kim *et al.*'s scheme with the optimal reversing measurement strength $p_r = p + D\bar{p}$ [20]. We find that our first modification [Fig. 13(b)] is obviously superior to Kim *et al.*'s scheme within a certain operation parameter range.

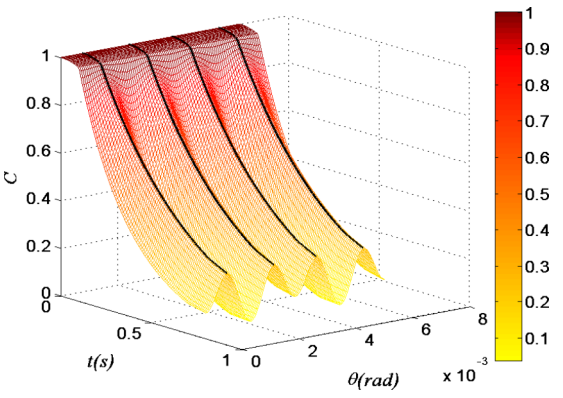

FIG. 15. (Color online) Concurrence evolution in the first modified scheme as a function of time t and θ. The black lines are optimum, and the corresponding $\theta_1 = 6\pi/25, \theta_2 = 19\pi/25, \theta_3 = 31\pi/25, \theta_4 = 44\pi/25$. $\gamma_1 = 1000, t_1 = 10^{-4}$ s, $\gamma_2 = 1000, t_2 = 6 \times 10^{-4}$ s, $\gamma_3 = 1000, t_3 = 10^{-1}$ s, and total time is 8×10^{-4} s. $a = 1.0$.

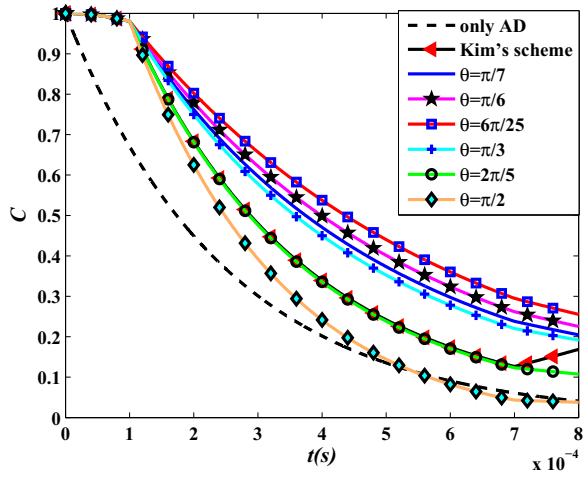

FIG. 16. (Color online) Concurrence as a function of t. The black dashed line represents the entanglement evolution under amplitude damping without any control, and $\gamma = 1000$. The black solid line represents the entanglement evolution in Kim *et al.*'s scheme with the optimal reversing measurement strength, $\gamma_1 = 1000, t_1 = 10^{-4}$ s, $\gamma_2 = 1000, t_2 = 6 \times 10^{-4}$ s, $\gamma_3 = 2077, t_3 = 10^{-1}$ s. The other six curves with $\theta = \pi/7, \theta = \pi/6, \theta = 6\pi/25, \theta = \pi/3, \theta = 2\pi/5$, and $\theta = \pi/2$ are the entanglement evolutions for modified scheme 1, $\gamma_1 = 1000, t_1 = 10^{-4}$ s, $\gamma_2 = 1000, t_2 = 6 \times 10^{-4}$ s, $\gamma_3 = 1000$, $t_3 = 10^{-1}$ s. $a = 1.0$.

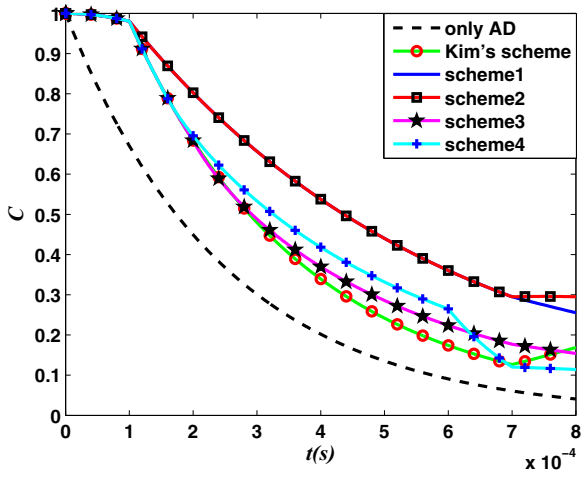

FIG. 17. (Color online) Concurrence as a function of t. The black dashed line represents the entanglement evolution under amplitude damping without any control and $\gamma = 1000$. The green solid line with circles represents the entanglement evolution in Kim *et al.*'s scheme with the optimal reversing measurement strength, $\gamma_1 = 1000, t_1 = 10^{-4}$ s, $\gamma_2 = 1000, t_2 = 6 \times 10^{-4}$ s, $\gamma_3 = 2077, t_3 = 10^{-1}$ s. The red solid line with squares represents the entanglement evolution in modified scheme 2 and is slightly better than the blue (dark gray) solid line (scheme 1). The pink line with stars represents modified scheme 3, and the time point for control is $t = 2 \times 10^{-4}$ s. The cyan line with pluses represents modified scheme 4, and the time points for control are $t_1' = 1.5 \times 10^{-4}$ s, and $t_2' = 6 \times 10^{-4}$ s. In our schemes, $\gamma_1 = 1000, t_1 = 10^{-4}$ s, $\gamma_2 = 1000, t_2 = 6 \times 10^{-4}$ s, $\gamma_3 = 1000, t_3 = 10^{-4}$ s. $a = 1.0$.

When $\theta = 2\pi/5$, the two concurrence evolution curves appear to overlap. When $\theta = \pi/2$, our first modification is inferior to Kim *et al.*'s scheme. In Fig. 17, we show concurrence evolution curves for the different modifications. All four modified schemes can protect quantum entangled states, and the modified scheme in Fig. 13(c) is relatively better than the other three modified schemes and Kim *et al.*'s scheme. To summarize, the unique operation used in Kim *et al.*'s scheme can be replaced with a rotational operation at a random time point during amplitude damping, which can reduce experimental complexity effectively.

V. CONCLUSION

In conclusion, we studied how to reverse the entanglement damping of the EBL state due to weak measurement and amplitude damping. In the weak-measurement-induced damping case, we demonstrated that entanglement of initial pure or mixed states can be protected through the combined action of unitary operation series. The numerical simulations indicate that this protocol can protect remote bipartite entanglement with a wide range of unitary operations. The key point here is that the fluctuations of the time interval, the operation parameters, and the duration time of the operations are all taken into consideration. The results show that these real factors only slightly affect the protection efficiency of the scheme. In the genuine amplitude-damping case, we presented four modified schemes to enhance the protection efficiency of Kim *et al.*'s scheme [20], and the bit-flipping operations in Kim *et al.*'s scheme are replaced with one or two rotational operations. The results indicate that the modified schemes can protect bipartite entanglement better than Kim *et al.*'s scheme, and the specific relation between the magnitude of system decoherence, the strength of the weak measurement, and the strength of the reversing measurement in Kim *et al.*'s scheme is not also needed. Our schemes are more tolerant of operation and time interval fluctuations, which makes these schemes more feasible.

ACKNOWLEDGMENTS

This work is supported by the National Natural Science Foundation of China (NSFC) under Grants No. 11274010, No. 11204002, and No. 11374085; the Specialized Research Fund for the Doctoral Program of Higher Education (Grants No. 20113401110002 and No. 20123401120003); the Key Project of the Chinese Ministry of Education (No. 210092, No. 211080); Anhui Provincial Natural Science Foundation under Grant No. 1408085MA16; the Key Program of the Education Department of Anhui Province under Grants No. KJ2012A020, No. KJ2012A244, and No. KJ2012A206; the "211" Project of Anhui University; the Talent Foundation of Anhui University under Grant No. 33190019; the personnel department of AnhuiProvince; and the Anhui Key Laboratory of Information Materials and Devices (Anhui University).

[1] M. A. Nielsen and I. L. Chuang, *Quantum Computation and Quantum Information* (Cambridge University Press, Cambridge, 2000).
[2] P. W. Shor, Phys. Rev. A **52**, R2493 (1995).
[3] A. M. Steane, Phys. Rev. Lett. **77**, 793 (1996).
[4] D. A. Lidar, I. L. Chuang, and K. B. Whaley, Phys. Rev. Lett. **81**, 2594 (1998).
[5] P. G. Kwiat, A. J. Berglund, J. B. Altepeter, and A. G. White, Science **290**, 498 (2000).
[6] L. A. Wu and D. A. Lidar, Phys. Rev. Lett. **88**, 207902 (2002).
[7] L. Viola, E. Knill, and S. Lloyd, Phys. Rev. Lett. **82**, 2417 (1999).
[8] J. R. West, D. A. Lidar, B. H. Fong, and M. F. Gyure, Phys. Rev. Lett. **105**, 230503 (2010).
[9] P. Facchi and S. Pascazio, Phys. Rev. Lett. **89**, 080401 (2002).
[10] P. Facchi, D. A. Lidar, and S. Pascazio, Phys. Rev. A **69**, 032314 (2004).
[11] S. Maniscalco, F. Francica, R. L. Zaffino, N. Lo Gullo, and F. Plastina, Phys. Rev. Lett. **100**, 090503 (2008).
[12] V. Weisskopf and E. Wigner, Z. Phys. **63**, 54 (1930).
[13] Q. Q. Sun, M. Al-Amri, and M. S. Zubairy, Phys. Rev. A **80**, 033838 (2009).
[14] A. N. Korotkov and K. Keane, Phys. Rev. A **81**, 040103 (2010).
[15] X. Xiao and M. Feng, Phys. Rev. A **83**, 054301 (2011).
[16] Z. X. Man, Y. J. Xia, and N. B. An, Phys. Rev. A **86**, 012325 (2012).
[17] X. Xiao and Y. L. Li, Eur. Phys. J. D **67**, 204 (2013).
[18] N. Katz *et al.*, Phys. Rev. Lett. **101**, 200401 (2008).
[19] Y. S. Kim, Y. W. Cho, Y. S. Ra, and Y. H. Kim, Opt. Express **17**, 11978 (2009).
[20] Y. S. Kim, J. C. Lee, O. Kwon, and Y. H. Kim, Nat. Phys. **8**, 117 (2012).
[21] J. C. Lee, Y. C. Jeong, Y. S. Kim, and Y. H. Kim, Opt. Express **19**, 16309 (2011).
[22] Q. Sun, M. Al-Amri, L. Davidovich, and M. S. Zubairy, Phys. Rev. A **82**, 052323 (2010).
[23] C. Q. Wang, B. M. Xu, J. Zou, Z. He, Y. Yan, J. G. Li, and B. Shao, Phys. Rev. A **89**, 032303 (2014).
[24] M. Al-Amri, M. O. Scully, and M. S. Zubairy, J. Phys. B **44**, 165509 (2011).
[25] Z. Y. Liao, M. Al-Amri, and M. S. Zubairy, J. Phys. B **46**, 145501 (2013).
[26] P. Dong, Z. Y. Xue, M. Yang, and Z. L. Cao, Phys. Rev. A **73**, 033818 (2006).
[27] W. K. Wootters, Phys. Rev. Lett. **80**, 2245 (1998).
[28] S. B. Zheng, Phys. Rev. A **68**, 035801 (2003).